

## MULTI-SPECIES EQUILIBRATION USING THERMAL LATTICE BOLTZMANN SIMULATIONS

Linda Vahala<sup>1</sup>, George Vahala<sup>2</sup> and Pavol Pavlo<sup>3</sup>

<sup>1</sup>*Dept. of Electrical & Computer Engineering, Old Dominion University, Norfolk, VA, USA*

<sup>2</sup>*Dept. of Physics, William & Mary, Williamsburg, VA, USA*

<sup>3</sup>*Institute of Plasma Physics, Association EURATOM/IPP.CR, Praha 8, Czech Republic*

### 1. Advantages of a Lattice Boltzmann Approach Over Conventional Methods for SOL

In designing codes to handle the scrape-off layer (SOL) and the divertor region, one must deal with the dynamical evolution of various fronts (e.g., heat, ionization, radiation..) for multi-species systems in complex geometry. The difficulty facing traditional computational approaches are formidable. For example, current work considers a coupled UEDGE-Navier Stokes solver for the strongly collisional (“fluid”) regime [1]. In weakly collisional regimes, a Monte Carlo (“kinetic”) approach is typically used. Thus the dynamic coupling of these codes is numerically stiff because of the disparate length and time scales involved in the fluid and kinetic representations, respectively. Moreover, even when treating the highly collisional regime, the neutrals have been assumed, for computational tractability, laminar and 2D. The extension of full 3D dynamics is also not straightforward. Now a major problem facing this standard CFD (computational fluid dynamics) approach is the accurate resolution of the nonlinear convective derivative  $\mathbf{v} \cdot \nabla \mathbf{v}$  -- i.e., the notorious nonlinear Riemann problem.

We have been pursuing an alternate computational approach, utilizing the thermal lattice Boltzmann model [TLBM, Ref. 2-6]. The potential advantages of moving to a linear kinetic representation on a lattice can not be overemphasized: (a) since one deals only with simple (linear) advection in kinetic space, the nonlinear Riemann problem of CFD is completely side-stepped. Moreover, the kinetic advection can be handled by simple shift operation using a Lagrangian representation. This results in a kinetic CFL of 1, so that no artificial (numerical) dissipation or diffusion is introduced into the solution; (b) the TLBM structure is ideal for multi-PE computer architectures. No saturation with PE’s has been seen, all the way to the 512 PE’s currently available on the T3E and the IBM-SP3; (3) TLBM is readily extended to 3D; and finally (4) TLBM can be used to span all ranges of collisionality : a simple BGK-collision operator for the highly collisional (fluid) regime, and a more sophisticated collision operator in the weakly collisional (Monte Carlo) regime. This unified representation has been gained at no computational speed reduction from standard CFD due to the ideal parallelizability of the TLBM code. This will gain will be further enhanced when the number of PE’s on the IBM-SP3 is increased from the present 512 to 2048 PE’s.

### 2. Discrete TLBM Representation and 2D Simulation Results

Here we report on 2D TLBM equilibration simulations in the highly collisional regime for heat fronts propagating in a neutral-plasma system. The discrete kinetic equation for the neutrals (‘1’)

$$N_{1p}(\mathbf{x} + \mathbf{c}_p, t + 1) - N_{1p}(\mathbf{x}, t) = -\frac{1}{\tau_1} [N_{1p}(\mathbf{x}, t) - N_{1p}^{eq}(\mathbf{x}, t)] - \frac{1}{\tau_{12}} [N_{1p}(\mathbf{x}, t) - N_{12p}^{eq}(\mathbf{x}, t)] \quad (1)$$

where  $\mathbf{c}_p$  is the kinetic velocity lattice vector and  $N_{1p}$  is the neutral distribution function.  $\tau_1$  is neutral-neutral relaxation time for to the ‘equilibrium’ distribution function  $N_{1p}^{eq}$ , while  $\tau_{12}$  is the neutral-ion relaxation time, with  $\tau_{12} \gg \tau_1$ . Similarly for the ion kinetic equation. Using Chapman-Enskog analysis, one recovers the full fluid conservation equations for mass, momentum and energy. If the collisional terms are dominant over the advection terms, Morse [7] has estimated that the temperature to velocity equilibration rates for the two species should scale as (where  $n_s, m_s$  are the density and mass of the sth species)

$$\frac{\tau_{\Delta\theta}}{\tau_{\Delta v}} \approx \frac{1}{2} \left( \frac{n_1 m_1 + n_2 m_2}{n_1 + n_2} \right) \left( \frac{m_1 + m_2}{m_1 m_2} \right) \geq 1 \text{ for } m_1 \neq m_2. \quad (2)$$

In our simulations, we consider a high temperature heat front in the ions interacting with a lower temperature front in the neutrals ( $T_2 = 1.2T_1$ ) in which both the ions and neutrals are turbulent because of the strength of the double velocity shear layers. The plasma and neutral layers and fronts are initially perpendicular to each other [see Fig. 1], with the neutrals being heavier and denser than the plasma [ $m_1 = 5m_2; n_1 = 3n_2$ ] and with initial vorticity  $\omega_2 = 2\omega_1$ . In the figures, the left frame is for the vorticity while the right frame is for the temperature at that time instant; while within each frame, the right plot is for the plasma and the left plot is that for the neutrals.

The vortex layers break up into clumps of individual vortices, with the plasma layers breaking up first – Fig. 2, at  $t = 1.5$  K TLBM time steps. The individual vortices of like sign then merge – as is evident for the plasma. The neutral layer is just breaking up at  $t = 1.5$  K, and the ion temperature front is undergoing significant perturbation (Fig. 2). By  $t = 3$  K, fig. 3, the neutral vorticity is very chaotic and its temperature front is undergoing significant perturbation. The ion temperature front has been broken up by the turbulence. By  $t = 7.35$  K, fig. 4, the ion and neutral vorticities are globally equilibrating, but the temperatures are still significantly different. Fine scale velocity equilibration has occurred by  $t = 10.5$  K, Fig. 5, while some global temperature similarities can be seen. Full temperature equilibration is close to being reached by  $t = 18.5$  K, Fig. 6. Thus the TLBM simulation ratio of the rate of temperature to velocity equilibration is approximately 1.76, in close agreement with Morse’s theoretical estimate of 2.4. The difference can be readily attributed to nonlinear effects that are neglected by Morse. In particular, we have found that for more turbulent initial conditions, the Morse estimate breaks down because of the importance of the nonlinear convective terms in the momentum and energy species equations.

Movies of the vorticity and temperature evolutions can be seen at the ODU web page <http://www.ece.odu.edu/~lvahala/2DTURB/>.

### Acknowledgements

The computations presented here were performed on the NERSC J90’ s and T3E. Special thanks to Nancy Johnston (NERSC) for providing the movie-making routines. Supported by DOE, and by GA CR grant# 202/00/1216.

### References

- [1] D. A. Knoll et. al., Phys. Plasmas **3** (1998) 422.
- [2] F. J. Alexander, S. Chen and J. D. Sterling, Phys. Rev. **E47** (1993) 2249.
- [3] P. Pavlo, G. Vahala and L. Vahala, Phys. Rev. Lett. **80** (1998) 3960.
- [4] G. Vahala, P. Pavlo, L. Vahala and N. Martys, Intl. J. Modern Phys. **C9** (1998) 1274.
- [5] G. Vahala, J. Carter, D. Wah, L. Vahala and P. Pavlo, to appear in *Parallel CFD99*
- [6] L. Vahala, D. Wah, G. Vahala, J. Carter and P. Pavlo, Phys. Rev. **E62** (July 1, 2000)
- [7] T. F. Morse, Phys. Fluids **6** (1963) 1420; **7** (1964) 2012.

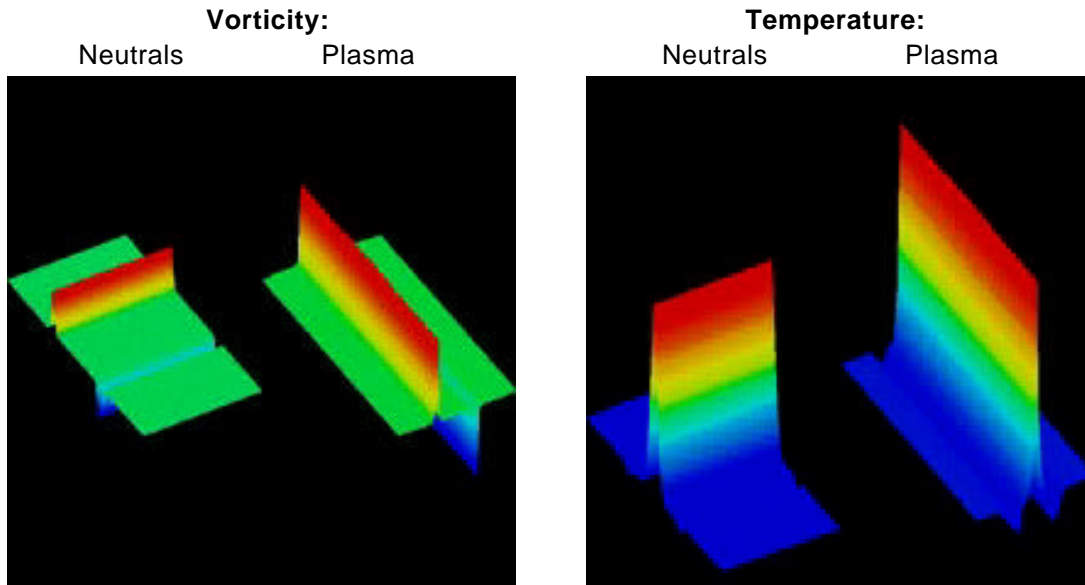


*Fig. 1. Vorticity and temperature at time  $t = 0$  (initial conditions).*

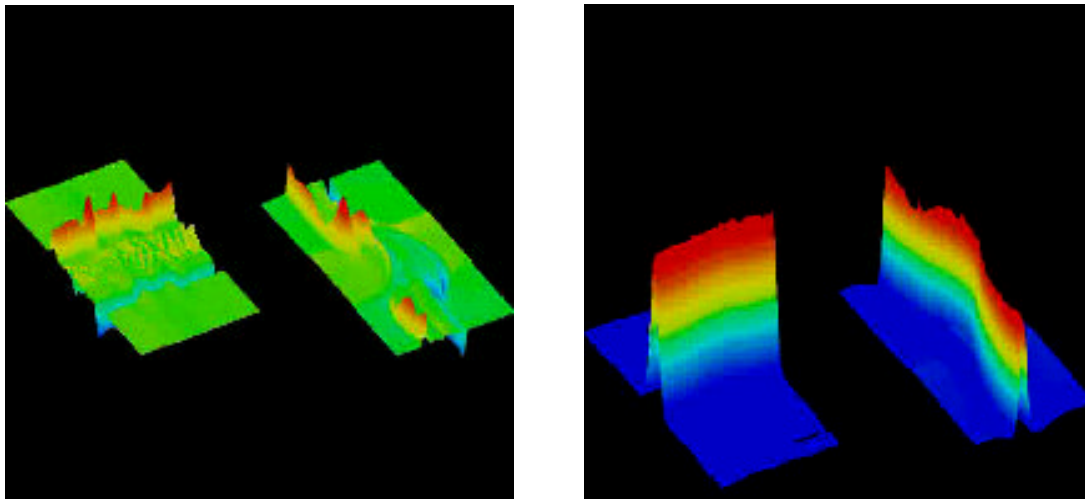


*Fig. 2. Vorticity and temperature at time  $t = 1.5K$ .*

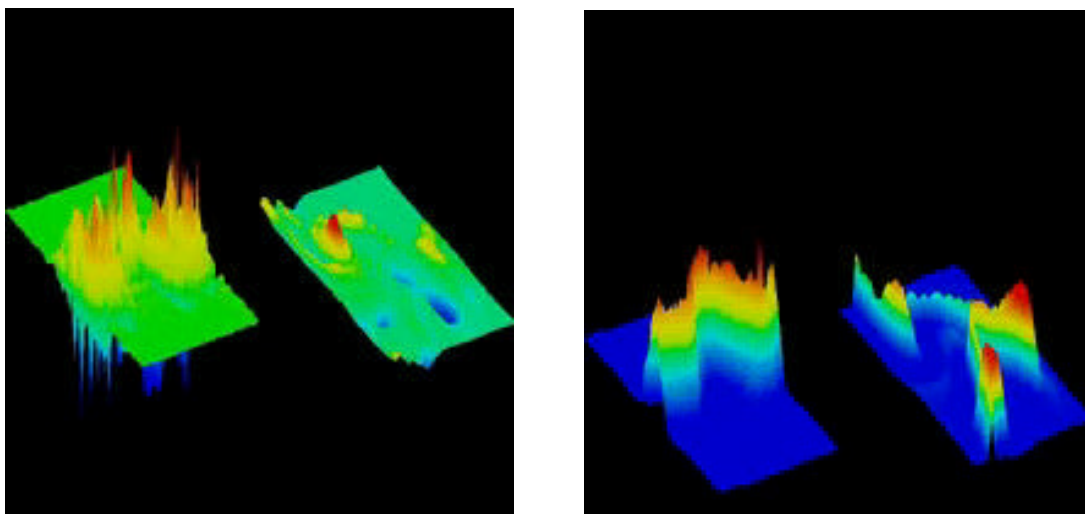


*Fig. 3.  $t = 3K$ .*

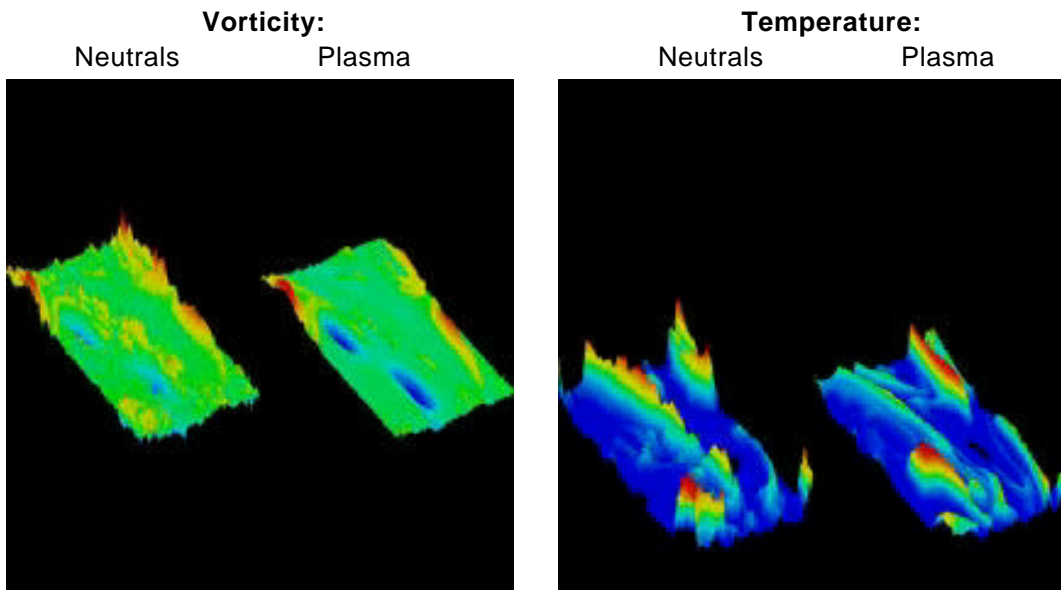


*Fig. 4. Vorticity and temperature at time  $t = 7.35K$ .*

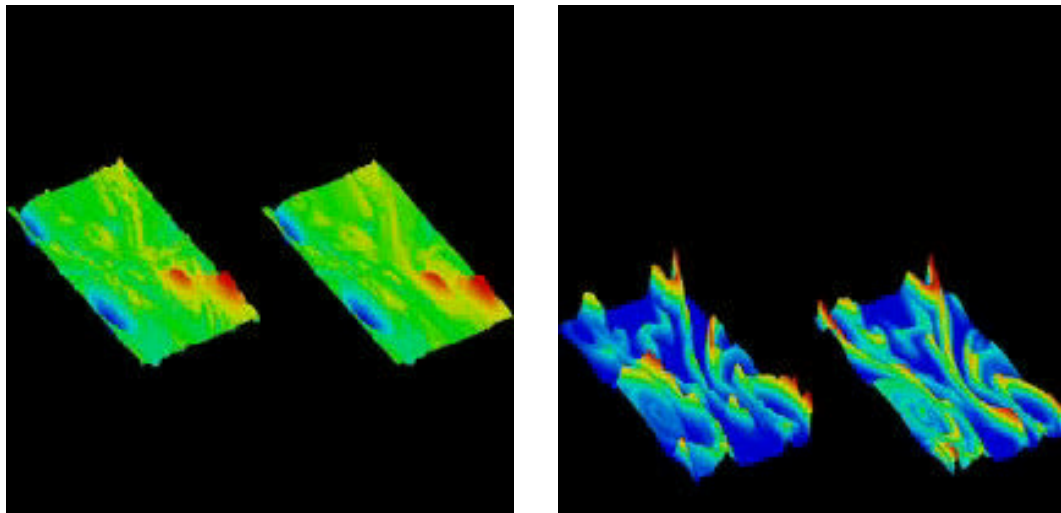


*Fig. 5.  $t = 10.5K$ .*

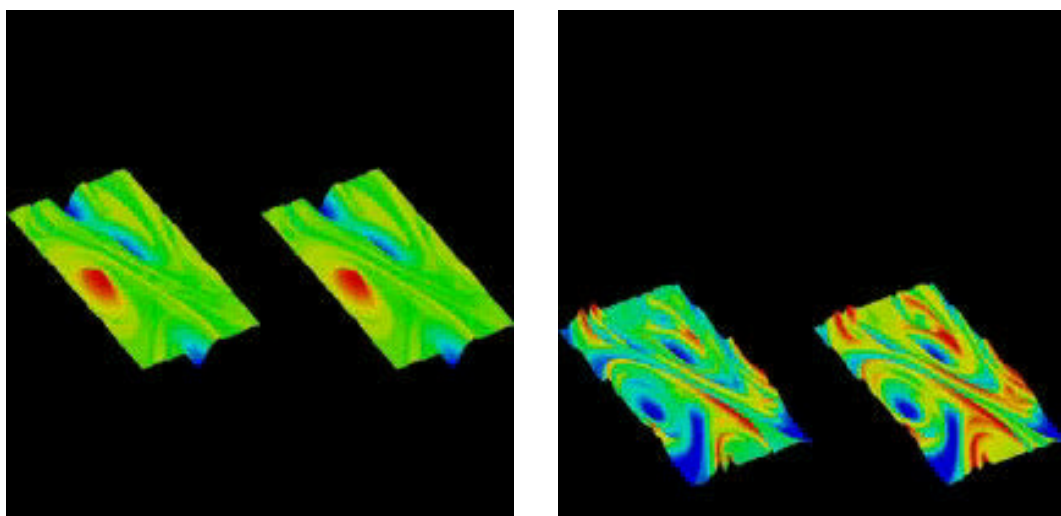


*Fig. 6.  $t = 18.5K$ .*